Report, Structural Analysis and Steel Structures Institute, Hamburg University of Technology, Hamburg, June, 2013

Pancake-type collapse—energy absorption mechanisms and their influence on the final outcome (complete version)

Nikolay Lalkovski

Dipl.-Ing., Structural Analysis and Steel Structures Institute, Hamburg University of Technology, Denickestr. 17, 21073 Hamburg, Germany

nikolay.lalkovski@tuhh.de, +49 40 42878-2435

Uwe Starossek

Prof. Dr.-Ing., Structural Analysis and Steel Structures Institute, Hamburg University of Technology, Denickestr. 17, 21073 Hamburg, Germany

starossek@tuhh.de, +49 40 42878-3976

ABSTRACT

Since the World Trade Center disaster in 2001, various theories have been proposed as to what caused the observed rapid collapse progression ending in the total collapse of both towers. According to the theory now widely accepted, the columns in the aircraft impact zone lost their load-bearing capacity due to the effects of fire. As a result, the upper part of the building fell over the height of at least one story. The resulting impact forces greatly exceeded the buckling load of the columns near the impact zone, which led to the release of a new portion of potential energy. It was also shown that the energy absorbed by the columns during buckling was significantly less than the potential energy released during this process. This led to the conclusion that the total collapse was inevitable once initial failure occurred.

However, there are some examples of buildings, in which the columns of an entire story failed and no collapse progression occurred. Such cases were observed in the 1995 earthquake in Kobe, Japan. There were also some failed controlled demolition attempts, in which a progressive collapse to be triggered by the destruction of vertical load bearing elements in lower levels did not occur. No significant deformations or damages of vertical elements were observed in these cases. This raises the question if there are energy absorption mechanisms other than column buckling that may play a role in the structural response to initial failure. Numerical simulations of simple representative systems of steel-framed buildings are presented showing that there are such mechanisms indeed and that column buckling is not the only possible way to absorb the energy at impact. These simulations are preceded by the description of an analytical approach that is based on a simplified model and gives first insights in the response and the modeling requirements of the structure.

1. INTRODUCTION

Losing one or more vertical load-bearing elements is among the most feared consequences of extreme events in high-rise buildings. The possible loss of a large floor area above the failed vertical elements is the reason why a growing number of building codes require an examination of the structural performance of important high-rise buildings following the instantaneous loss of one or more columns. It has to be shown that the loads of the floors above the damaged part of the structure are able to find alternate paths to the supports.

However, the chances of preventing collapse progression obviously diminish with growing number of initially destroyed vertical elements. Even if the loads can be transferred to the remaining columns (by bending and/or catenary action in the floors or by a hat truss), for a certain number of initially destroyed columns the remaining columns can no longer support the load and start to buckle progressively in a zipper-type manner (Starossek, 2007). This can be particularly critical for the first story of high-rise buildings where the number of columns is reduced due to utilization requirements, as was the case in the Murrah Federal Building in Oklahoma City. The horizontal spread of column buckling across a floor has been recognized as the most critical event in a multi-story steel-framed building (Lim, 2004). Once this occurs, a collision of the upper part of the structure with the structure below or – if it is the first story that is initially affected by column buckling – the ground is inevitable. In most cases the structure will be damaged beyond repair at this point. Nevertheless, concerning the occupants' lives, developing strategies for arresting the collapse in this early stage is still an important issue. To do this, a clear understanding of the possible deformation patterns and failure mechanisms that develop at impact is needed.

In cases of collisions that involve kinetic energies large enough to cause significant plastic deformations, it is intuitively expected that these deformations are concentrated in the vicinity of the impact zone. The model proposed by Bazant and Zhou (2002) is based on this assumption. However, in the case of a building structure colliding with the ground or another hard surface, this may not be true. To understand why, a closer look at some distinctive features of the problem is needed. The structure may be viewed as a body with a high portion of hollow space colliding with a more or less rigid surface. Most of the mass of this body is concentrated in the floors – elements oriented parallel to the impact surface and flexible in the direction of the resulting inertia forces. The columns contain the remaining portion of the mass. They have high initial stiffness in vertical direction up to the point in time when significant buckling deformations start to develop.

Thus, the assumption that the falling structure behaves like a rigid body cushioned by plastically buckling columns in the vicinity of the impact surface is only correct when the floor deformations are negligible. In fact, as will be demonstrated, the opposite may be the case: a significant part of the kinetic energy may be dissipated in the floors.

2. SIMPLIFIED MODEL

First, a simplified model is developed to gain first insights into the behavior of the structure at impact and to derive threshold values for various structural properties that have influence on the ensuing deformation pattern. It is based on elementary considerations neglecting secondary effects. Its purpose is not to exactly calculate the system behavior (although relatively good results are achieved), but to lead to a better understanding of the problem and thus help to develop solutions.

An approach to calculating the dynamic plastic behavior of an impulsively loaded beam was presented by Jones (1989). This approach will be adopted and modified to describe the problem at hand. The adequacy and limitations of the proposed simplified model are later tested in numerical simulations and discussed.

2.1 *Assumptions*

2.1.1 *Initial damage*

It is assumed that a sufficient portion of the columns in one story of a steel-framed building is damaged to trigger a horizontal spread of column buckling across the whole floor area so that a collision with the ground or the lower structure becomes inevitable. This portion depends on the structural configuration and loading. For instance, in a building with a regular plan, the failure of a corner column and its two adjacent columns on the periphery will in many cases be sufficient to trigger progressive column buckling.

The cause of the initial damage can vary (e.g., fire, malicious action) and is of no interest here. A possible tilt of the falling structure, which can develop if the initially destroyed columns lay asymmetrically in plan, is neglected here and a constant vertical velocity over the cross section of the building is assumed at impact.

2.1.2 *Impact surface*

The properties of the impact surface have a significant effect on the magnitude of the impact forces and their time history. This surface is considered here to be rigid, which seems realistic in case the structure collides with the ground after the first story is damaged and the cushioning effect of the forming rubble pile is negligible. It seems reasonable or at least safe to first ignore the influence of this pile, whose properties are difficult to predict.

If the damaged story is at a higher level, it can still initially be assumed that all deformations remain confined to the falling upper part of the structure when it is weaker than the lower part. If then the upper part is analyzed assuming impact with a rigid body below, the calculated impact force as a function of time can be used in a subsequent dynamic calculation to check whether significant deformations develop in the lower part of the structure. If this is shown not to be the case, then the initially made assumption of a rigid impact surface is proven acceptable. This approach is similar to the widely used Riera method for designing nuclear power plant shells for aircraft impact, where it is assumed that the shell does not deform and the whole kinetic energy is dissipated in the destruction of the aircraft (Riera, 1968). Only the behavior of the falling structure will be investigated in this study. The lower structure will be the subject of future work.

2.1.3 *Material model*

The elastic response is neglected and a rigid-perfectly plastic material model is used. It can easily be shown that the maximum elastic energy that can be stored in the system is only a small fraction of the kinetic energy in an impact with, say, 6 m/s. Thus, the use of a rigid-perfectly plastic material model is justified with respect to the energy balance. However, the elastic response, especially in the early stages after impact, may have an influence on the deformation pattern that develops after impact. This aspect, as well as the effect of the strain hardening, which is also neglected, will be checked subsequently in more refined numerical simulations.

Furthermore, the material is assumed to be strain rate insensitive. The incorporation of strain rate effects in the model will be the subject of future work.

2.1.4 *Transverse shear effects and shear-moment interaction*

While shear forces in a beam are rarely important in static problems, they can have a considerable influence in the response to dynamic loading. This is especially true if the loading has significant high frequency content as is the case here. The influence of the excited higher eigenmodes with shorter wave lengths is more noticeable in the shear forces than in the bending moments (Jones, 1989). Transverse shear effects will be taken into account in this rigid-plastic model. The dynamic shear force has its maximum at the beam support points. When the plastic shear capacity is exceeded there, a plastic shear hinge is inserted into the model. The longitudinal extension of this shear hinge is idealized as infinitesimally short, such that a discontinuity in the transverse displacement field is assumed to occur at this point. While this assumption is obviously not correct for the behavior on a local level, it is acceptable for capturing the effect on the global beam behavior, which is the main focus of this study.

Beams with I-cross section are of main interest here. The contribution of the web to the plastic bending moment capacity for such a cross section is relatively small (in the order of 10 to 15% for most I-beams used in practice). Thus, even if the web is utilized to 100% in shear, the plastic moment capacity will not be significantly reduced. For this reason, shear-moment interaction is neglected without causing major errors in the results.

2.1.5 *Small displacements*

Only small displacements are considered in the model. As will be demonstrated by the subsequent numerical simulations, even large beam deflections have negligible effect as long as catenary action does not play a role.

2.1.6 *Column behavior*

The column behavior is crucial for the overall deformation mode and, therefore, should be accounted for as accurately as possible. It can generally be said that a statically loaded column can tolerate only small plastic compressions without significant loss in axial capacity. Only columns with relatively low slenderness ratio whose axial load-displacement curve remains approximately constant over the first few cm are considered in the simplified model. It will be shown that the plastic column compressions that occur at impact can be limited to such low values by relocating plastic zones to other parts of the structure that can experience large deformations without endangering the global stability.

The column loading in the problem at hand is of is not of static but of dynamic nature. A study presented in the following will demonstrate that this has favorable effects on the axial load-displacement curve of the column. It is important to point out, however, that the derivations and conclusions in later chapters do not depend on these favorable effects, under the afore made assumption of a relatively sturdy column.

Fig. 1 shows a comparison of load-displacement curves for a dynamically loaded imperfect column obtained from finite element simulations in the time domain. The upper end of the column is moved downwards with various constant velocities to obtain the various curves. For comparison, the static response is also shown. It was obtained by neglecting inertia forces in the corresponding simulation.

In this study, the column has a square 0.36 m x 0.36 m box cross section with a wall thickness of 0.02 m. The other column parameters and the assumed initial imperfection are indicated in Fig. 1. A bilinear material model with Young modulus of 210,000 N/mm², strain hardening modulus of 960 N/mm², Poisson ratio of 0.3, yield strength of 240 N/mm², and density of 7,850 kg/m³ is used. No strain rate effects are considered. The calculations are performed with ANSYS, using elements of the type BEAM188. This element type is well suited for large strain nonlinear applications. It is obvious from the use of beam elements that effects of local instability (plate buckling) were not considered in this study.

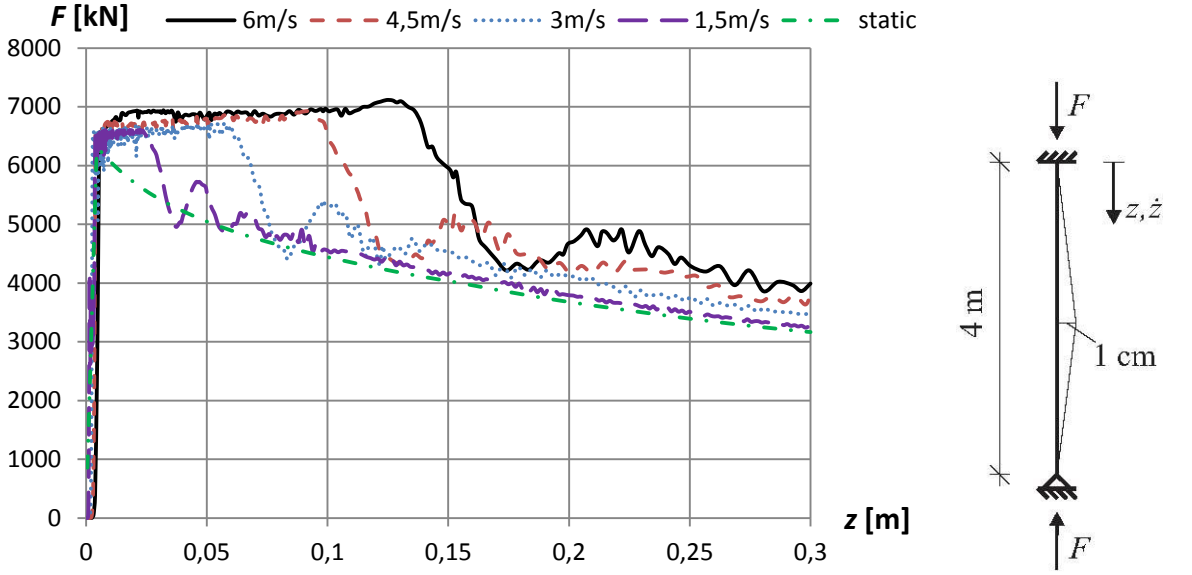

Figure 1: Load-displacement curves for a dynamically loaded imperfect column for different imposed constant vertical velocities of the upper end

Fig. 1 shows the differences between static and dynamic column buckling and the effect of the magnitude of the imposed velocity. In all cases, the maximum value of the axial reaction force is approximately the same (the slightly higher values in the dynamic cases are explained below). But while in the static case it starts to drop immediately after the maximum value is reached, an almost constant maximum value of the axial force is initially maintained in the dynamic cases until a certain threshold value of vertical displacement is reached. This threshold value depends on the imposed velocity. As to be expected, the differences between the static case and the dynamic cases become smaller for smaller velocities.

The differences between static and dynamic column buckling result from the stabilizing effect of the lateral inertia forces acting on the column in the dynamic cases. At the beginning of a dynamic simulation, as the upper end is forced to move downwards with constant velocity, the column center point starts to accelerate horizontally in the direction of the initial imperfection. As the lateral displacement grows with time, so does the corresponding sway force and it becomes ever more difficult for the inertia forces to compensate for it. Finally, a point is reached where the sway force starts to dominate over the stabilizing effect of the horizontal inertia forces. This point is marked by a steep drop of the axial reaction force to what would approximately be its static value for the corresponding vertical displacement. After that, dynamic effects become negligible as the column buckles sideways with an approximately constant velocity. Due to the delay in the development of buckling deformations, leading to a localization of plastic zones, the initial axial strains in the dynamic cases are somewhat higher. This, combined with the non-zero strain hardening modulus of the material, explains the slightly higher values of the maximum axial force in the dynamic cases.

There is an important common feature in all dynamic cases, which is not quite obvious from Fig. 1. It is easily recognized in Fig. 2, however, where the same data is presented in a slightly different way. The load curves are here shown as functions of time instead of displacement. The steep drop in the axial force occurs at about the same time for all velocities. The curves end at different times because in all cases the upper end of the column was moved over the same distance (0.3m).

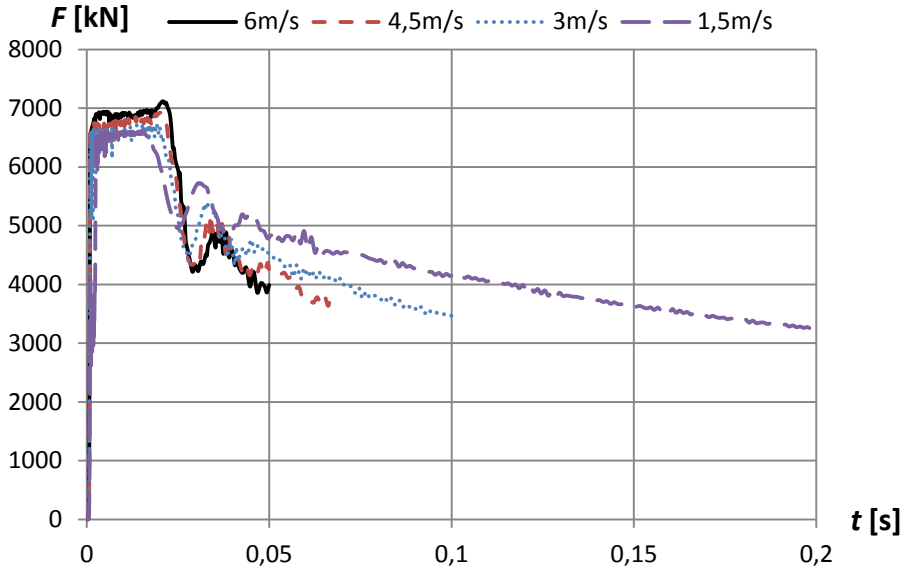

Figure 2: Load as a function of time for the dynamic cases from Fig. 1

Another numerical simulation was performed on the column from Figs. 1 and 2 to further study this feature. At time $t = 0$, the column was suddenly loaded with an axial force corresponding to the yield strength of its cross section and constant over time. Fig. 3 shows the displacement of the loaded upper end as a function of time. At about $t = 0.02$ s, there is a change in the sign of the curvature indicating that the loaded end starts to accelerate in the direction of the applied force. In other words, the column loses its ability to support the applied force at $t = 0.02$ s, which qualitatively matches the result from Fig. 2.

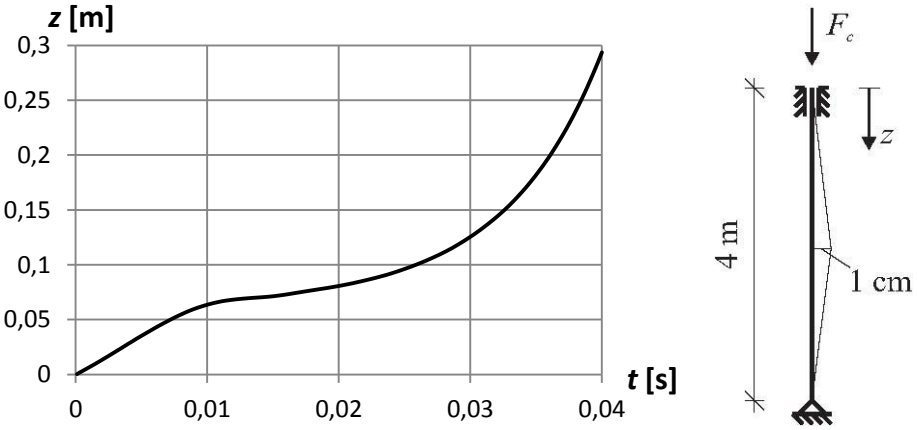

Figure 3: Vertical displacement over time for a column suddenly loaded to its yield capacity

The following conclusion can be drawn. When a column with a given imperfection is suddenly loaded to its bearing capacity due to an impact, the time over which it can support the applied load is independent of the impact velocity. In contrast, the vertical displacement

over which such a column can maintain a constant force varies depending on the impact velocity. It should be noted that these findings might not apply to large plastic compressions where local buckling, neglected here, will occur. More studies, where the different parameters are varied, are needed to confirm and better explain these findings.

A rigid-plastic load-displacement characteristic is assumed for the column of the simplified model. It follows from the preceding discussion that this (when stabilizing lateral inertia effects are disregarded) is only admissible if the column is relatively sturdy and experiences only small plastic compressions. Further details will become clear later.

2.2 *Considered structure and simplification steps*

The model is developed for a two dimensional steel frame with any number of stories and bays. Fig. 4 shows the considered structure and the simplification steps explained below. The simplification mainly consists in reducing the structure to one inner column with tributary beam elements and then further to one spring-mounted beam element. Because the model assumes only axial loading and no bending in the columns, it is applicable to inner columns, and to outer columns only if the beam-column connections have no moment resistance. No bending in the inner columns will occur if all connections have the same rigid-perfectly plastic moment-rotation characteristic, which is one of the assumptions described below.

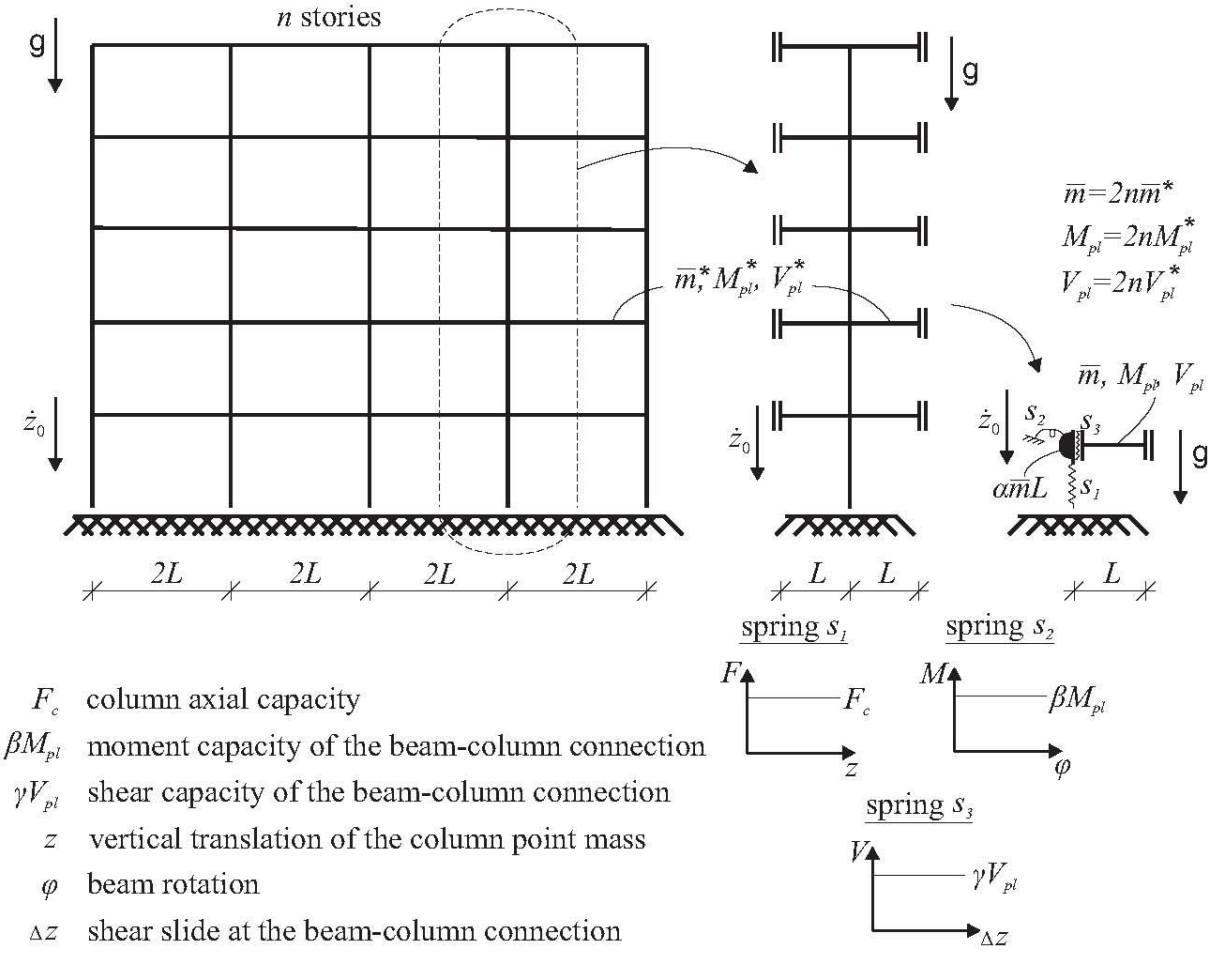

Figure 4: Two dimensional steel frame impacting a rigid surface with initial velocity $\dot{z}_0$ and simplification steps

The moment and shear capacity of the beam-column connection are taken as a portion of the moment and shear capacity of the beam cross section (factors $\beta \leq 1$ and $\gamma \leq 1$, respectively). The mass of the column is taken as a portion of the beam mass including the contributions from slabs and payload (factor α, usually a value between 0.05 and 0.1). It is assumed that all horizontal elements have the same constant cross section and consist of the same material and mass constantly spread along their length.

The column cross section is first taken to be constant along the entire height. After the model is presented, it will be shown how also a piecewise variable column cross section can be accounted for. The axial force in the column resulting from the inertia forces during impact increases in downward direction, with abrupt changes at the beam connection points. Thus, for a cross section constant over the entire height, plastic deformations in the column can only develop in the lowest story. Because elasticity is ignored, the column segment above the first floor and extending to the top (called the upper column segment) can essentially be viewed as a rigid body and only the effect of its inertia is of interest in this model. (A study which will be presented elsewhere has shown that neglecting the elasticity of the column leads to conservative results for the plastic compression of the lowest-story column.) The mass of the plastically deforming lowest-story column segment is lumped to the mass of this rigid body.

Furthermore, all beams, should they deform plastically, will do so simultaneously because of the assumed rigidity of the upper column segment to which they are connected. Therefore, all beams can be lumped into a single one. Its properties are derived as the sum of the properties of all beams connected to the considered column. In the following explanations, the word "beam" denotes the half beam appearing in the last simplification step in Fig. 4.

The rigid-plastic springs s_2 and s_3 shown in the last simplification step represent the moment and shear connections, respectively, of the beam to the column. Spring s_1 representing the plastically compressed column segment in the lowest story has been explained above. All three springs are initially taken to be infinitely ductile. Then, in order for the obtained results to be correct, the calculated ductility demand on each of the three springs and on plastic hinges that may form along the beam has to be smaller than the ductility supply. Exceeding the ductility supply for the different springs leads to different corresponding collapse modes. Some of these collapse modes are shortly mentioned in the following chapter.

2.3 *Model of the column-beam structure under impact*

The main idea is that, depending on the capacities of the three rigid-plastic springs shown in Fig. 4, one, two, or all three of them yield at impact, which leads to a specific deformation mode. This mode, in turn, determines the inertia force distribution in the system. Because the deformation mode and the inertia force distribution are interrelated, it is expedient to first assume a deformation mode. The constellation of spring capacities that leads to the assumed mode can then be determined.

According to the rigid-plastic hypothesis for the structural material and the assumption of a rigid impact surface, the axial force in the lowest-story column will immediately reach the plastic capacity of the column cross section F_c and will initially remain constant. Depending on the value of F_c, and, as will be shown below, also on the value of γV_{pl}, plastic moment hinges at the beam ends may or may not develop at impact. In the first case, the beam will start to rotate in addition to its downward translation. This case will be considered first. The possibility of plastic shearing in the beam-column connection is considered later.

2.3.1 *Initially combined rotation and vertical translation of a beam remaining straight*

2.3.1.1 *No plastic shearing in the beam-column connection*

It is first assumed that the beam remains straight (no plastic moment hinges develop along the length, only at the ends) and no plastic shearing occurs at the connection to the column. The conditions under which these assumptions are valid will be derived below. In the considered case, the system has only two possible degrees of freedom – the rotation and the vertical displacement of the center of gravity are used in the following derivations. The situation is shown in Fig. 5.

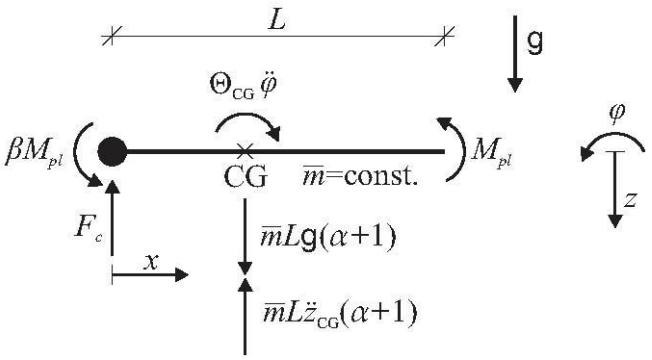

Figure 5: Simplified structure with forces and moments acting on it for the case of initially combined rotation and vertical translation without plastic shearing

Equilibrium of vertical forces yields the vertical acceleration of the center of gravity:

$$\ddot{z}_{CG} = g - \frac{F_c}{\bar{m}L(\alpha+1)}$$

It is clear that the structure will only decelerate if $F_c > \bar{m}Lg(\alpha+1)$. This condition is obviously fulfilled, as the column is able to support the gravity load and will usually have significant reserves. Moment equilibrium about the center of gravity yields the angular acceleration:

$$\ddot{\varphi} = \frac{12M_{pl}(\alpha+1)(\beta+1) - 6F_cL}{\bar{m}L^3(4\alpha+1)}$$

Now, in order for the plastic moment hinges at the beam ends to get active under the action of the inertia forces, as was initially assumed, the angular acceleration has to be non-zero and negative. This yields the first condition for beam rotation:

$$F_c > \frac{2M_{pl}(\alpha+1)(\beta+1)}{L}$$

If the axial capacity of the column is smaller than this value the motion of the beam will be a pure downward translation, and the beam will dissipate no energy in bending. This case will be considered later.

Now, considering further the case that a rotation does occur, taking into account the initial conditions:

$\dot{z}_{CG,0} = \dot{z}_0$

$\dot{\varphi}_0 = 0$

$z_{CG,0} = 0$

$\varphi_0 = 0,$

the system motion can now be fully described.

$$\dot{z}_{CG}(t) = -\left(\frac{F_c}{\bar{m}L(\alpha+1)} - g\right)t + \dot{z}_0$$

$$z_{CG}(t) = -\left(\frac{F_c}{\bar{m}L(\alpha+1)} - g\right)\frac{t^2}{2} + \dot{z}_0 t$$

$$\dot{\varphi}(t) = \frac{12M_{pl}(\alpha+1)(\beta+1) - 6F_cL}{\bar{m}L^3(4\alpha+1)}t$$

$$\varphi(t) = \frac{6M_{pl}(\alpha+1)(\beta+1) - 3F_cL}{\bar{m}L^3(4\alpha+1)}t^2$$

For the later derivations it will be more convenient to express the vertical displacement, velocity, and acceleration as functions of x and t (no horizontal displacements occur for small rotations). Taking into account that:

$$z(x,t) = z_{CG}(t) - \varphi(t)(x - x_{CG})$$

$$\dot{z}(x,t) = \dot{z}_{CG}(t) - \dot{\varphi}(t)(x - x_{CG})$$

$$\ddot{z}(x,t) = \ddot{z}_{CG}(t) - \ddot{\varphi}(t)(x - x_{CG})$$

after some calculation, it follows that:

$$z(x,t) = \left(\frac{g}{2} + \frac{3M_{pl}(\beta+1) - 2F_cL}{\bar{m}L^2(4\alpha+1)}\right)t^2 + \frac{3F_cL - 6M_{pl}(\alpha+1)(\beta+1)}{\bar{m}L^3(4\alpha+1)}t^2x + \dot{z}_0 t$$

$$\dot{z}(x,t) = \left(g + \frac{6M_{pl}(\beta+1) - 4F_cL}{\bar{m}L^2(4\alpha+1)}\right)t + \frac{6F_cL - 12M_{pl}(\alpha+1)(\beta+1)}{\bar{m}L^3(4\alpha+1)}tx + \dot{z}_0$$

$$\ddot{z}(x,t) = g + \frac{6M_{pl}(\beta+1) - 4F_cL}{\bar{m}L^2(4\alpha+1)} + \frac{6F_cL - 12M_{pl}(\alpha+1)(\beta+1)}{\bar{m}L^3(4\alpha+1)}x$$

Due to the fact that the beam deceleration has its maximum at the support, it is obvious that motion will first come to an end there. The time t_1, at which the motion at the support ceases, is obtained from the condition $\dot{z}(x = 0, t = t_1) = 0$.

$$t_1 = \frac{\dot{z}_0}{\frac{4F_cL - 6M_{pl}(\beta+1)}{\bar{m}L^2(4\alpha+1)} - g}$$

This point in time marks the end of the first phase of motion. Here, the velocity profile will change from a combination of vertical translation and rotation to a pure rotation about the support, which means that new functions will describe the system motion in the following

second phase. The derivations for the first phase of motion will be valid if it can be shown that the calculated plastic compression of the column $z(x = 0, t = t_1)$ does not cause any significant loss in its axial capacity. If this is the case, the calculation can continue. As will be shown below, at time $t = t_1$ the dynamic support reaction (equal to the contact force at the column base) will suddenly drop from F_c to a lower value, which is consistent with the fact that plastic compression of the column ceases at this point in time.

The remaining kinetic energy in the system at $t = t_1$ will be dissipated during the following second phase of motion. The system has now only one degree of freedom as the beam remains stationary at the support. The velocity and displacement at the end of the first phase of motion are the initial conditions for the second phase of motion. Fig. 6 shows the beam during the second phase of motion. Θ_0 is the mass moment of inertia about the support.

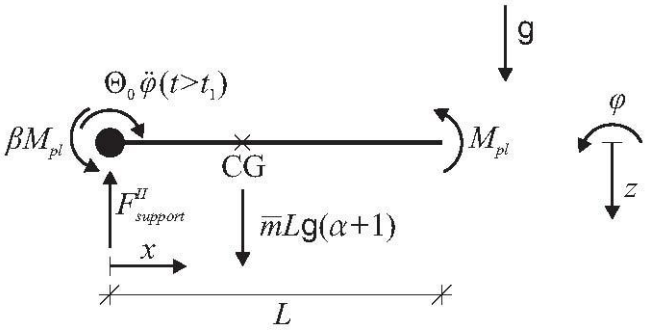

Figure 6: Beam rotating about the stationary support point during the second phase of motion

The angular acceleration is obtained from a moment equilibrium about the support:

$$\ddot{\varphi}(t > t_1) = \frac{3M_{pl}(\beta + 1) - 1{,}5\bar{m}gL^2}{\bar{m}L^3}$$

Integration with respect to time, taking into account the initial conditions for the second phase of motion:

$$\dot{\varphi}(t_1) = -\frac{\dot{z}(x = L, t = t_1)}{L}$$

$$\varphi(t_1) = -\frac{z(x = L, t = t_1) - z(x = 0, t = t_1)}{L}$$

yields the angular velocity and the rotation.

$$\dot{\varphi}(t > t_1) = \frac{3M_{pl}(\beta + 1) - 1{,}5\bar{m}gL^2}{\bar{m}L^3}(t - t_1) + \dot{\varphi}(t_1)$$

$$\varphi(t > t_1) = \frac{3M_{pl}(\beta + 1) - 1{,}5\bar{m}gL^2}{2\bar{m}L^3}(t - t_1)^2 + \dot{\varphi}(t_1)(t - t_1) + \varphi(t_1)$$

If required, the vertical displacement, velocity, and acceleration can now be obtained as functions of x and t in the same way as this was done for the first phase of motion. For example, using the rotation calculated above:

$$z(x, t > t_1) = -\varphi(t > t_1)x + z(x = 0, t = t_1)$$

The dynamic support reaction during the second phase of motion is calculated from equilibrium condition for the vertical forces. Taking into account that the resultant inertia force acts at a distance $2/3L$ from the support and has the value $\Theta_0\ddot{\varphi}(t > t_1)/(2/3L)$ yields:

$$F_{support}^{II} = \frac{1{,}5M_{pl}(\beta+1)}{L} + \bar{m}gL(\alpha + 0{,}25)$$

Obviously, a discontinuity in the support reaction as a function of time occurs at time t_1. The reason is the sudden change in the inertia force distribution along the beam length at this time point (due to the change in the displacement pattern). Apart from this discontinuity, the acceleration and the support reaction remain constant in each of the two phases of motion.

Fig. 7 shows the beam at times 0, t_1 and t_2. At time t_2 the beam rotation about the support ceases, which marks the end of the second phase of motion. At this point in time no kinetic energy is left in the system, and the reaction force at the support drops to its static value.

Figure 7: Beam in different phases of motion

Time t_2 is obtained when the angular velocity for the second phase of motion $\dot{\varphi}(t > t_1)$ is set to zero ($\dot{\varphi}(t_2 > t_1) = 0$).

$$t_2 = \frac{\dot{\varphi}(t_1)\bar{m}L^3}{1{,}5\bar{m}gL^2 - 3M_{pl}(\beta+1)} + t_1$$

All derivations above are based on the condition that the rotating beam remains straight and no plastic shearing occurs. The conditions under which this initial assumption remains statically admissible are derived in the following.

During the first phase of motion, the shear force in the beam at $x = 0$, where it has its maximum, is obtained integrating the inertia and gravity loads over the beam length:

$$V(x=0) = \int_0^L \bar{m}(g - \ddot{z})\,dx = \frac{F_c L + 6M_{pl}\alpha(\beta+1)}{L(4\alpha+1)}$$

Remember that in order for beam rotation to occur, a condition requiring a minimum value for F_c has to be fulfilled. This condition was derived at the beginning, and is repeated here for convenience:

$$F_c > \frac{2M_{pl}(\alpha+1)(\beta+1)}{L}$$

Substituting this condition for F_c in the expression for $V(x=0)$ (this expression was obtained assuming beam rotation) yields:

$$V(x=0) > \frac{2M_{pl}(\beta+1)}{L}$$

The beam will only rotate if the plastic shear capacity of its connection allows this minimum value for $V(x=0)$ to develop there. This yields a second condition for beam rotation, requiring a minimum value for the plastic shear capacity:

$$\gamma V_{pl} > \frac{2M_{pl}(\beta+1)}{L}$$

This condition, combined with the one requiring the minimum value for F_c, guarantees beam rotation. This rotation may be combined with plastic shearing at the support depending on whether $\gamma V_{pl} < V(x=0)$. The results obtained so far remain valid as long as the value for $V(x=0)$ is smaller than or just equal to the plastic shear capacity γV_{pl}, meaning that no plastic shearing occurs. Otherwise, another case – that of plastic shearing occurring in addition to the beam rotation – must be considered. This is done in the next subchapter.

The conditions for one more initial assumption for the present case – that the beam remains straight – have to be derived. These are the conditions under which the bending moment caused by the calculated inertia force distribution does not exceed the plastic moment capacity anywhere along the beam. Now, the shear force as a function of x during the first phase of motion (during this phase the shear force is constant with respect to time) is:

$$V(x) = \frac{\partial M}{\partial x} = \int_0^x \bar{m}(\ddot{z}(\bar{x}) - g)d\bar{x} + V(x=0) =$$

$$\frac{3F_cL - 6M_{pl}(\alpha+1)(\beta+1)}{L^3(4\alpha+1)}x^2 - \frac{4F_cL - 6M_{pl}(\beta+1)}{L^2(4\alpha+1)}x + \frac{F_cL + 6M_{pl}\alpha(\beta+1)}{L(4\alpha+1)}$$

The bending moment has a local extremum at $x = L$ as $V(x=L) = 0$. The question whether this extremum is a maximum or a minimum is resolved by the sign of the second derivative of the bending moment with respect to x at $x = L$.

$$\frac{\partial V(x=L)}{\partial x} = \frac{\partial^2 M(x=L)}{\partial x^2} = \frac{2F_cL - 6M_{pl}(2\alpha+1)(\beta+1)}{\bar{m}L^2(4\alpha+1)}$$

If this term is > 0, there will be a local minimum in the bending moment function at $x = L$. This will be the case if:

$$F_c > \frac{3M_{pl}(2\alpha+1)(\beta+1)}{L}$$

In this case, there will be an yield violation somewhere along the length of the beam. Consequently, in order for all derivations based on the straight-beam hypothesis to remain valid, F_c must not exceed the value on the right side of the inequality above.

If F_c is greater than this value, and no plastic shearing occurs, a plastic moment hinge will develop at a certain point along the length of the beam, leading to a kink there, which will then move towards $x = L$ (Jones, 1989). However, in most structural configurations to be found in practice, F_c does not reach values large enough to cause a kink in the rigid-plastic beam. Even if F_c does reach such values in some rare cases, a second condition, requiring a minimum plastic shear capacity γV_{pl} in order for a kink in the beam to develop, is likely to be violated. This second condition, obtained in the same manner as the minimum plastic shear capacity for beam rotation, requires that:

$$\gamma V_{pl} > \frac{3M_{pl}(\beta + 1)}{L}$$

In summary, both conditions for a kink in the beam will seldom be simultaneously fulfilled. Therefore, this case is considered practically irrelevant, and will not be studied further here.

2.3.1.2 *Plastic shearing in the beam-column connection*

If γV_{pl} is greater than the minimum plastic shear capacity required for beam rotation but smaller than $V(x = 0)$, a plastic shear slide will occur at the support point in addition to the beam rotation. (Of course, this will only happen if the local ductility allows it. Otherwise the beam will simply shear off at its connection to the column. In this case, the floors will fall on top of each other leading to a destruction scene typical for a pancake-type collapse.) If a plastic shear slide can develop, a discontinuity in the vertical displacement will occur at the beam-column connection. The beam and the column can now be analyzed independently from each other, because the plastic shearing will always last longer than the plastic column compression. This can be explained by the following consideration. In the case of shear yielding at the connection, the force decelerating the beam at $x = 0$ decreases, while the total force decelerating the column mass increases. This, in turn, means that the motion of the beam at $x = 0$ will last longer if plastic shearing occurs. The motion of the column, on the other hand, will last shorter in this case.

Fig. 8 illustrates the situation at impact. The acceleration of the column mass $\ddot{z}_c$ is readily obtained from equilibrium of the vertical forces on the column, and thus describing its motion now becomes a simple task without need of further explanations.

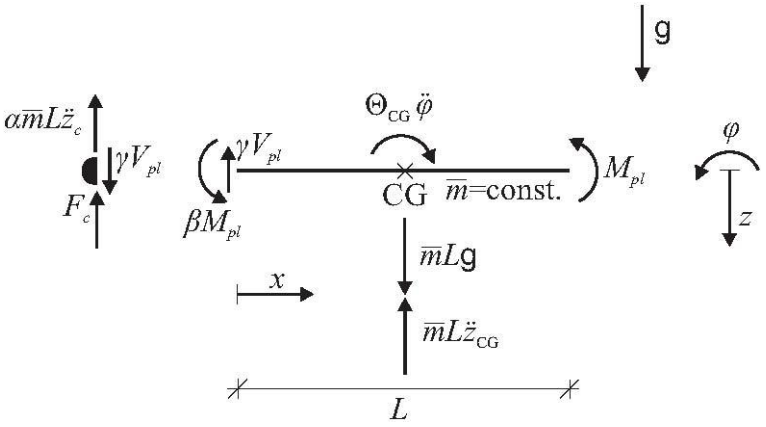

Figure 8: Initially combined rotation and vertical translation with plastic shearing in the beam-column connection – situation at impact

The dynamic response of the beam can be obtained using the approach presented for the case without plastic shearing, simply setting $\alpha = 0$ and replacing F_c by γV_{pl} for the first phase of motion – until plastic shearing ceases. The size of the plastic shear slide in the connection is equal to the difference between column displacement and beam displacement at $x = 0$.

2.3.2 *Pure downward translation of a beam remaining straight*

Pure downward translation will occur if one or both of the conditions for beam rotation (requiring minimum values for F_c and γV_{pl}) is violated. Fig. 9 shows the situation. The possible energy absorption mechanisms in this case are plastic compression of the columns in the lowest story and plastic shearing in the beam-column connection.

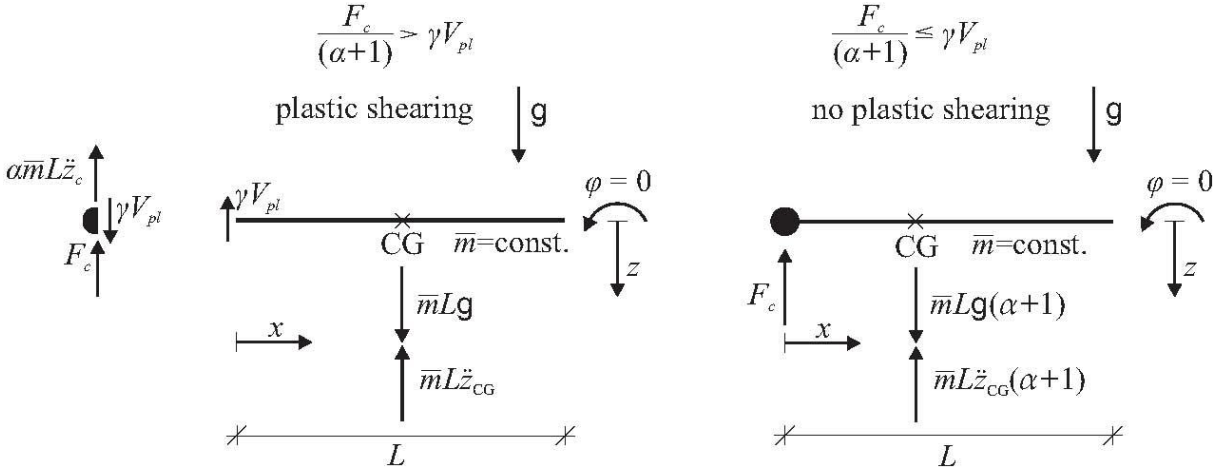

Figure 9: Pure downward translation of a straight beam with or without plastic shearing depending on the value γV_{pl}

The latter will occur if the shear force in the beam at $x = 0$, where it has its maximum, exceeds the value γV_{pl}. Taking into account that the inertia loading is now constantly spread along the beam length, the shear force in the beam column connection is calculated to:

$$V(x = 0) = \frac{F_c}{\alpha + 1}$$

For both cases – with and without plastic shearing – the accelerations can be easily calculated from equilibrium of the vertical forces. Time integration taking into account the initial conditions leads then to the solution for the velocity and displacement.

The amounts of energy which can be dissipated by both plastic shearing and plastic column compression are relatively small. Plastic shear slides that can be tolerated by the beam-column connection, if this is the case at all, will in most practical cases be in the order of only a few centimeters. The same can be said about the plastic compressions that can be tolerated by most columns without significant loss in axial capacity.

All in all, the case of pure downward translation, where the beams dissipate no energy in bending, is the most unfavorable with regard to chances of arresting the collapse.

2.3.3 *Summary of the different cases*

For a given structure, Fig. 10 shows the process of determining the deformation mode developing at impact in the form of a flowchart. Note that this deformation mode depends only on the properties of the structure, and not on the initial velocity. Once the deformation mode is determined, the dynamic response for the particular case can be obtained using the approach presented above.

According to the simplified model, plastic compression of the lowest-story column occurs in all cases, because this is the part of the rigid-plastic structure which comes in direct contact with the rigid surface. It has to be mentioned here that due to the column elasticity, disregarded in the simplified model, there may be cases where yielding of the lowest-story column occurs either delayed or not at all. The conditions under which these cases occur are derived and explained in detail elsewhere. What can generally be said is that disregarding column elasticity always leads conservative results for the amount of plastic compression in the lowest-story column.

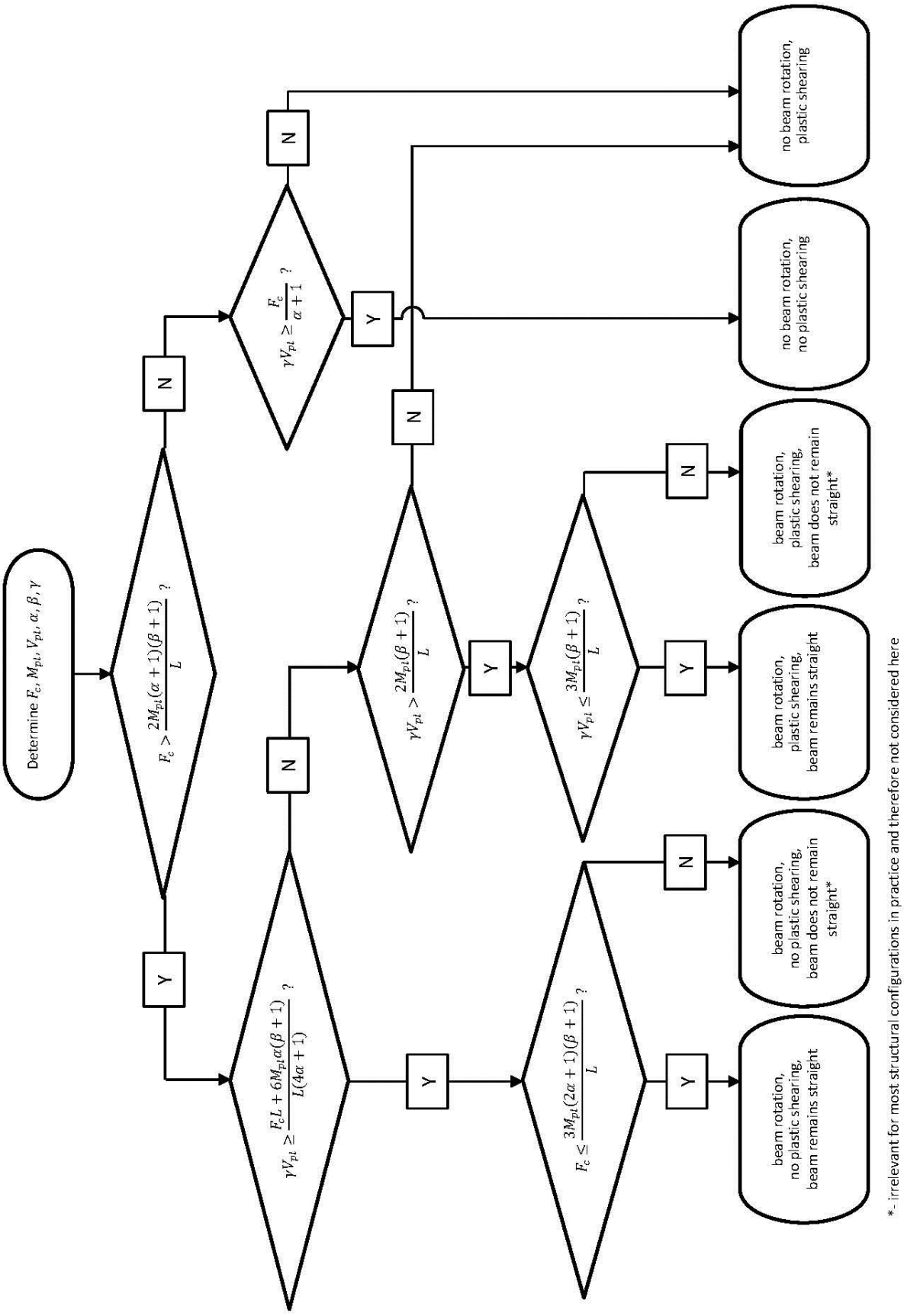

Figure 10: Flowchart for determining the deformation mode at impact for a given structure (plastic compression of the lowest-story column occurs in all cases)

2.4 *Implementation of a piecewise variable column cross section in the simplified model*

In the case of a variable column cross section, a slight modification in the presented simplified model is needed if the column capacity is exceeded somewhere along the height. Fig. 11 demonstrates how this can be handled.

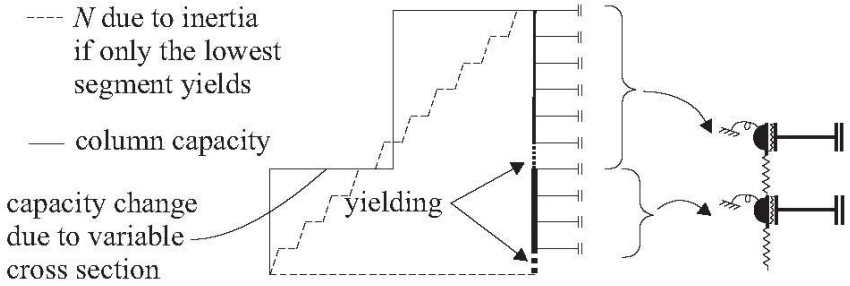

Figure 11: Column with a piecewise variable cross section along the height

Consider a column with a change in cross section, somewhere along the height, impacting a rigid surface. The dashed line indicates the normal force distribution if only the lowest column segment yields. At the bottom, it corresponds to the axial capacity of the lowest column segment. The abrupt changes result from the shear forces transmitted by the beams to the column at each story level. The solid line is the column capacity along the height. It can now easily be established whether the dashed line penetrates the solid line at the point of cross-sectional change, which would indicate yielding also of the column segment at this location (see Fig. 11). Again, the column segments above this location would not yield (as long as no further change of capacity occurs). The axial capacity at this location can be used to adjust the normal force distribution above the point of cross-sectional change. The same method applies when further cross-sectional changes occur. Fig. 11 also shows how the model is modified to take into account the additionally yielding column segment.

It should be noted that in the different sections of the structure divided by the yielding column segments different deformation modes can develop.

3. NUMERICAL SIMULATION RESULTS AND COMPARISON WITH THE SIMPLIFIED MODEL

Numerical simulations were performed to assess the adequacy of the simplified model. The results of one simulation, where many of the described effects occur, are presented and compared with the predictions of the simplified model.

Fig. 12 shows the analyzed system, which represents a symmetric one-bay two-column 7-story frame. The simulation is performed with ANSYS. The material model is the same as the one used for the simulations in Figs. 1 and 2. Columns and beams are modeled using beam elements of the type BEAM188. The beam-column connections have no moment resistance. They are modeled to yield in shear at a force of 700 kN. To do this, elements of the type NONLIN39 are used to connect the beams to the columns in the vertical direction. These elements have a bilinear characteristic with a very high initial stiffness up to the force of 700 kN. From then on, the force remains constant over the displacement. On the right end of the beams, the rotations are blocked and the displacements in horizontal and vertical direction are unrestrained. The horizontal displacements are left unrestrained to eliminate possible catenary effects in the model.

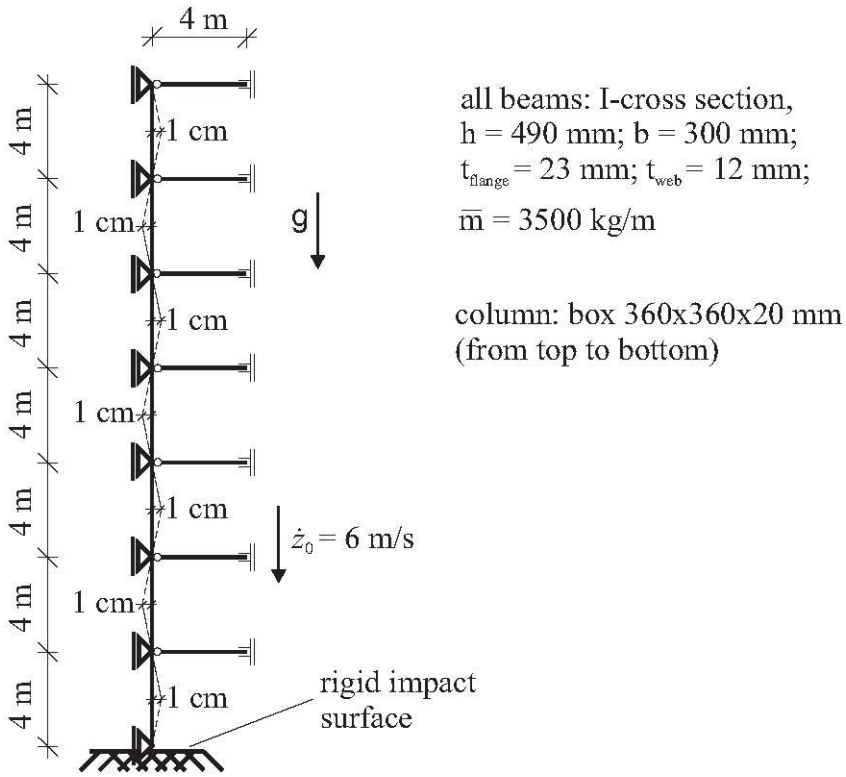

Figure 12: Analyzed 7-story structure

In reality, such effects will develop to some extent, depending on the lateral constraints and the horizontally accelerated mass, and will be implemented in the simplified model in the future.

The dashed line shows the assumed column imperfection. The simply supported beams are loaded by self weight to 30% of their plastic capacity ($\overline{m}$ = 3500 kg/m). The beam mass, constantly spread along the length, is taken into account by an increased density of the material used for the beams. The normal force due to gravity load acting in the lowest column section is 1,040 kN, which is about 16% of the column capacity. This utilization ratio due to characteristic gravity loads is not unusual for columns in high-rise buildings, which are also part of the lateral load resisting system.

An impact velocity of 6 m/s is assumed, which approximately corresponds to a free fall over half the height of a story. It is thereby considered that the columns in the initially affected story, which buckle progressively after the initial damage, will dissipate some energy before impact. Furthermore the forming pile of debris, assumed as rigid here, will have a certain thickness, which reduces the falling distance up to impact. Therefore a free fall over one full story height seems unrealistic.

Fig. 13 shows the contact force at the column base as a function of time as calculated by ANSYS and predicted by the simplified model. The deformation patterns of the simplified model in three distinctive points of time are also shown.

The solution was obtained using implicit Newmark time integration with a variable time step with a minimal value of 10^{-5} s. The time integration was performed approximately up to the point when no plastic zone was active within the structure and the contact force fell to its static value. This time, predicted by the simplified model to be 0.25 s, was confirmed in the simulation. Because no damping was defined, some elastic vibrations were left in the system at the end, which is deemed without importance.

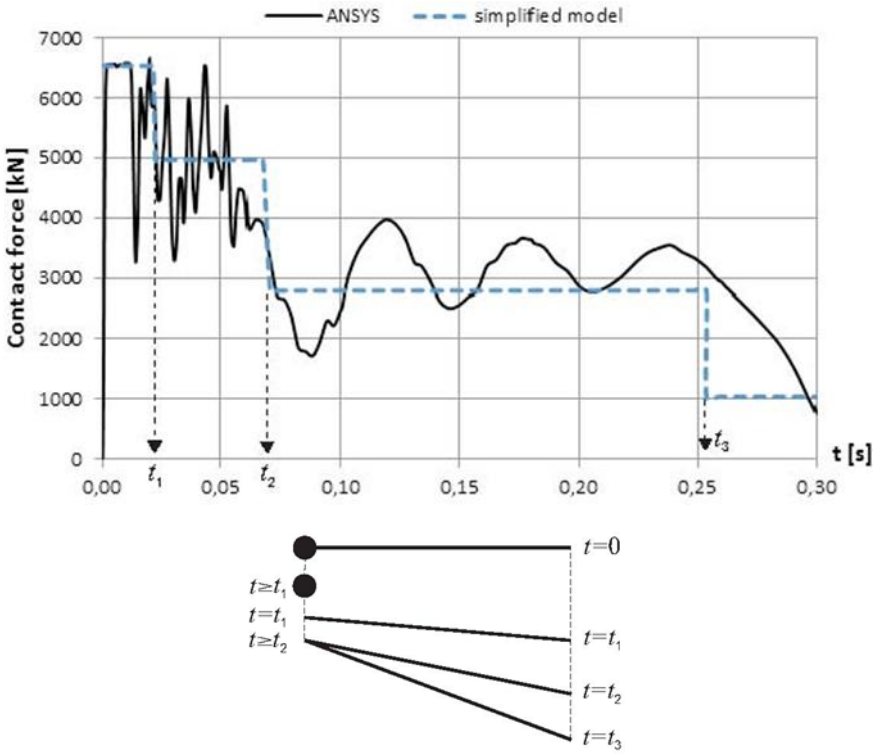

Figure 13: Contact force as a function of time

Three phases of motion are predicted by the simplified model up to the point when the contact force drops to its static value. These three phases can also be recognized in the numerical result for the contact force, which, apart from some high-frequency oscillations is well approximated by the simplified model.

In the first phase of motion, the column mass (about 6 t) is decelerated from 6 to 0 m/s. The column yield force of about 6500 kN is almost immediately reached at impact. Furthermore, the shear capacity of the beam-column connections and the moment capacity of the beam are exceeded and shear slides and plastic rotations start to develop. While in the simplified model this happens immediately at impact and simultaneously in all beams, some delay, especially for the upper beams occurs in the numerical model. This delay is due to the elastic wave propagation in the column, which is neglected in the simplified model. The first phase of motion ends when the lowest-story column stops to deform plastically. This occurs at t_1 = 0.022 s in the simplified model and at about 0.012 s in the numerical simulation. Again, this difference in time can be explained by the time delay due to elastic wave propagation in the column. The vertical forces transmitted by the beams to the column reduce the total force with which the column is decelerated. When these forces act delayed, then the total deceleration force immediately after impact is larger and the column comes to rest earlier thereby reducing the time of plastic compression. Hence elasticity is favorable here since not all the beam shear forces reach their maximum values immediately. According to the simplified model, the plastic compression of the column is 0.069 m. Only about half of this value is reached in the numerical simulation.

The second phase of motion comes to an end when the plastic shearing in the beam-column connections stops (while the plastic rotations in the beams continue). The contact force during this phase is 4,960 kN (7 x 700 + 60), resulting from the column weight of 60 kN and the plastic shear forces transmitted by the beams to the column. The simplified model predicts a total shear slide of about 0.13 m at the beam-column connection. According to the numerical simulation, this value is 0.10 m. The high-frequency oscillations in the contact force between

times t_1 and t_2 in the numerical result are due to undamped longitudinal vibrations in the column, left after the plastic compression of the lowest story has ceased.

The third phase of motion ends, when the plastic rotation of the beams stops. The maximum beam rotation according to the simplified model is 0.208 (vertical deflection: 0.83 m). The numerical result for the beam rotation is 0.225 (vertical deflection: 0.90 m).

Apart from the energy dissipated by the column, which is low anyway, the simplified model captures the energy distribution relatively well for this particular case. Most of the energy is dissipated in plastic beam bending: about 57% according to the simplified model and 72% according to the numerical simulation. The plastic shear hinges dissipate about 25% of the total energy according to the simplified model and 20% in the numerical simulation. The rest – about 18% in the simplified model and 8% in the numerical simulation is dissipated by the column. The elastic energy stored in the system in the numerical simulation is negligibly small.

4. CONCLUSIONS

It was demonstrated that the progressive collapse of a building structure impacting the ground or the lower part of the structure after the loss of one story is not inevitable. A simplified model, neglecting secondary effects, was described. Analysis based on this model shows that the building mass is decelerated in several consecutive phases in which the column force reduces stepwise, provided the column survives the first and most critical phase of motion. Most of the impact energy is dissipated in the beam-column connections and beams, which develop plastic shear slides and plastic moment hinges. The exposure of the columns is thus reduced and the prevention of collapse progression made possible.

Future efforts to improve the building performance in case of collapse initiation should concentrate on reducing the energy demand on the column at this very early stage so that the amount of damage it sustains is limited to a minimum. Developing beam-column connections with the ability to sustain large deformations in shear, maintaining a constant, well predictable force, and ensuring plastic rotation capacity in the beams are steps in this direction. Changes in column cross section along the height should be designed such that column yielding at impact occurs at as many points along the height as possible. In this way, plastic deformations in the columns are distributed along the height of the building instead of allowing them to concentrate in the lowest story only.

It remains to be clarified to what extent the findings here can be applied within the limits of economic design. By doing this, a more favorable deformation mode, in which most of the energy is dissipated by the beams, can be achieved in the extreme case of an impact with the ground or the lower structure. In this mode, plastic deformations are spread more evenly across the building volume and the energy absorption capacity of the structure is utilized to a higher degree. The limiting factor in this case will be the rotational capacity of the beam cross sections.

In the past, most improvement proposals concentrated on the idea of using vertical shock absorbers in some or all stories. Such shock absorbers would be activated when the columns buckle and maintain a relatively constant force in the order of magnitude of the column capacity (Starossek, 2009). The floors were considered to be rigid masses. As demonstrated by the simplified model, plastic shear slides and/or plastic moment hinges in the beams develop when the reaction forces acting on the beams immediately after impact exceed a certain value. After a short time, the motion at the point of support stops and the remaining kinetic energy must be dissipated solely by the beams. Thus, if vertical shock absorbers are

used, their maximum forces should remain small enough not to cause plastic deformations in the beams. This somewhat limits their effectiveness. If, on the other hand, the shock absorbers are designed to develop large forces, plastic beam deformations result. In this case, the shock absorbers would only be active for a short time and most of the energy would have to be dissipated by the beams.

REFERENCES

ANSYS, Inc., (2009). ANSYS Release 12.0 Documentation.

Bazant, Z. and Zhou, Y., (2002). "Why Did the World Trade Center Collapse? – Simple Analysis". Journal of Engineering Mechanics, 128(1), 2-6.

Jones, N., (1989). "Structural Impact". Cambridge University Press.

Lim, J., (2004). "Progressive Collapse Analyses of Steel Framed Moment Resisting Structures". Doctoral Thesis. The Pennsylvania State University.

Riera, J., (1968). "On The Stress Analysis of Structures Subjected to Aircraft Impact Forces". Nuclear Engineering and Design 8 (1968), 415-426, North-Holland Publishing Comp., Amsterdam.

Starossek, U., (2007). "Typology of Progressive Collapse". Engineering Structures 29, Nr. 9, 2302-2307.

Starossek, U., (2009). "Progressive Collapse of Structures". Thomas Telford, London.